

The required minimum transconductance is given as:

$$g_m = \frac{1}{R_p}$$

Where R_p is the loss of the resonator and g_m is the transconductance of the core circuit [6].

The oscillation frequency of the oscillator can be estimated from the below mentioned expression:

$$\omega_{osc} \approx \frac{1}{\sqrt{L_1 + L_2 + L_3(C_1 + C_2)}}$$

The M_1 and M_2 with gate width of 36 μm are used for core circuit. The ω_{osc} will vary due to change in inductor values which depends on the switch selection either for 40GHz or for 80GHz.

B. Circuit Design

The transistors with shorted drain and source are used as varactors whose labels are C_1 and C_2 with 20 μm gate width. The M_3 and M_4 are worked as source follower for output termination. The gate width for source follower transistors is 20 μm . The output capacitors C_3 and C_4 with source follower are having value of 800fF with metal insulated metal (MIM) design configuration. These capacitors are designed with OA top metal layer which is less lossy as compare to other metal layers. The capacitance value of different widths of transistor with respect to tuning voltage is depicted in Fig. 2. Fig. 3 shows quality factor of varactors with respect to tuning voltage. This is the reason for selection of 20 μm gate width for wider tuning range.

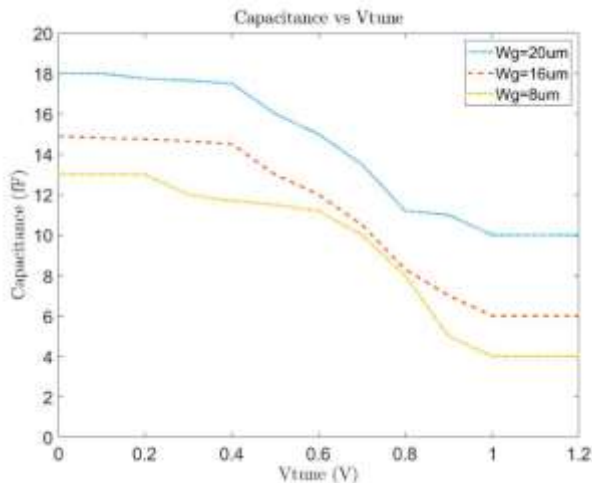


Fig. 2. Variation of different gate width capacitances w.r.t tuning voltage

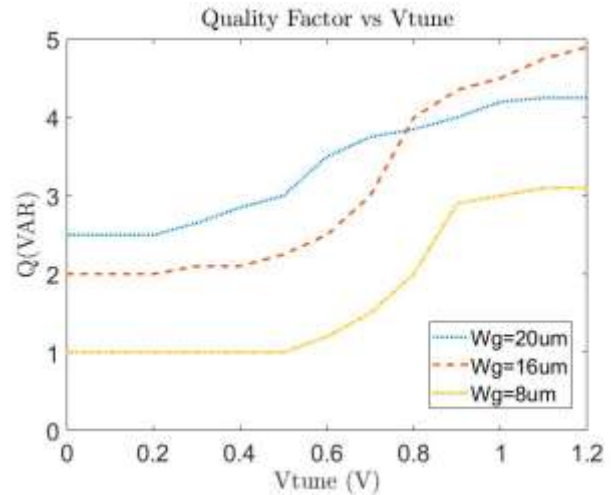


Fig. 3. Varactors quality factor w.r.t tuning voltage variation

The core circuit is leading the switching circuit which is used for inductor switching. The 1st switch V_{sw1} is used for small oscillator with large inductor whose output frequency is 40 GHz and 2nd switch V_{sw2} utilizes the small inductor for high frequency oscillation with 80 GHz output. The M_5 and M_6 are used with gate width 20 μm for switching purpose.

The L_1 , center tapped inductor is designed separately with inductance of 40 pH and it is utilized in both VCO modes. The L_2 and L_3 are designed in stacked fashion for saving die area with values of 20 pH and 70 pH respectively.

The micro-photograph of the dual band VCO with probing pads is portrayed in Fig. 4 with a die area of 500 x 560 μm^2 .

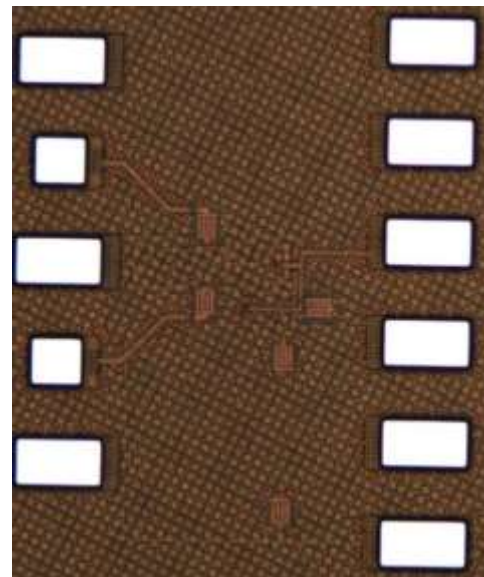


Fig. 4. chip microphotograph of proposed dual band VCO

III. EXPERIMENTAL RESULTS

The proposed VCO is simulated with EM momentum setup in ADS design tool. The schematic is designed in Spectre (Cadence) with 65nm CMOS process design kit. The two different oscillation frequencies are observed with switched VCO characteristics. 80GHz with output power of 0dBm is

achieved with switch 1 and inductor L_2 , sensitivity of VCO w.r.t time is shown in Fig. 4 with a tuning range of 4GHz .

Table 1: Performance Comparison with Prior Dual Band VCOs

Ref #	[10]	[11]	[12]	This work
Freq (GHz)	45/60	24/60	38/19	40/80
Tech.	0.25um BiCMOS	0.13um CMOS	0.25um BiCMOS	65nm CMOS
PN@1M (dBc/Hz) (@10M)	-99/-93	-120/-114	-106.8/-112	-94/-81
Pdc (mW)	32.5/17.5	24/11	105.6/69.3	42
FOM _{PN}	158/156	177/176	178/180	170/163

$$FOM_{PN} = -L(\Delta f) + 20 \log \frac{f_{osc}}{\Delta f} - 10 \log \frac{P_{dc}}{1mW}$$

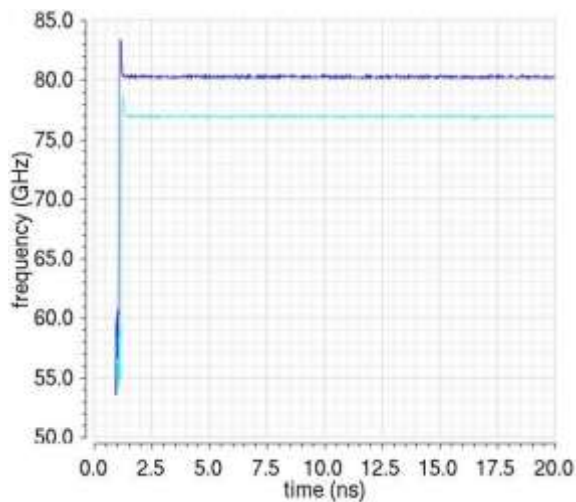


Fig. 4. Output Frequency sensitivity w.r.t time for 80GHz VCO

Similarly, 40GHz can be obtained with switch 2 and inductor L_1 as described in Fig. 5. The tuning range for 40GHz is 1GHz and it can also be observed in Fig. 5.

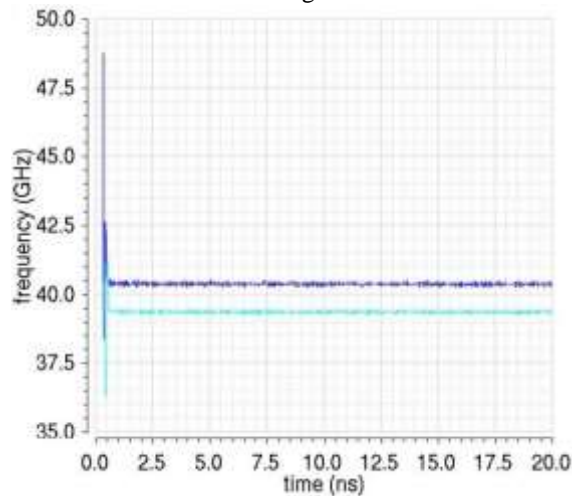


Fig. 5. Output Frequency sensitivity w.r.t time for 40GHz VCO

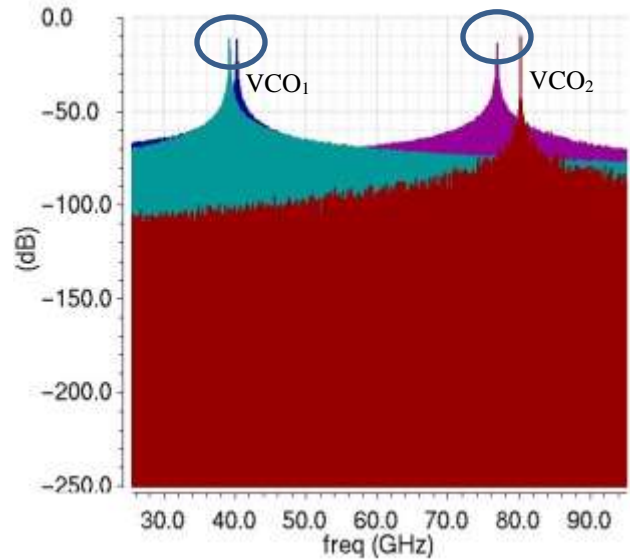


Fig. 6. Frequency spectrum for both VCO₁ and VCO₂

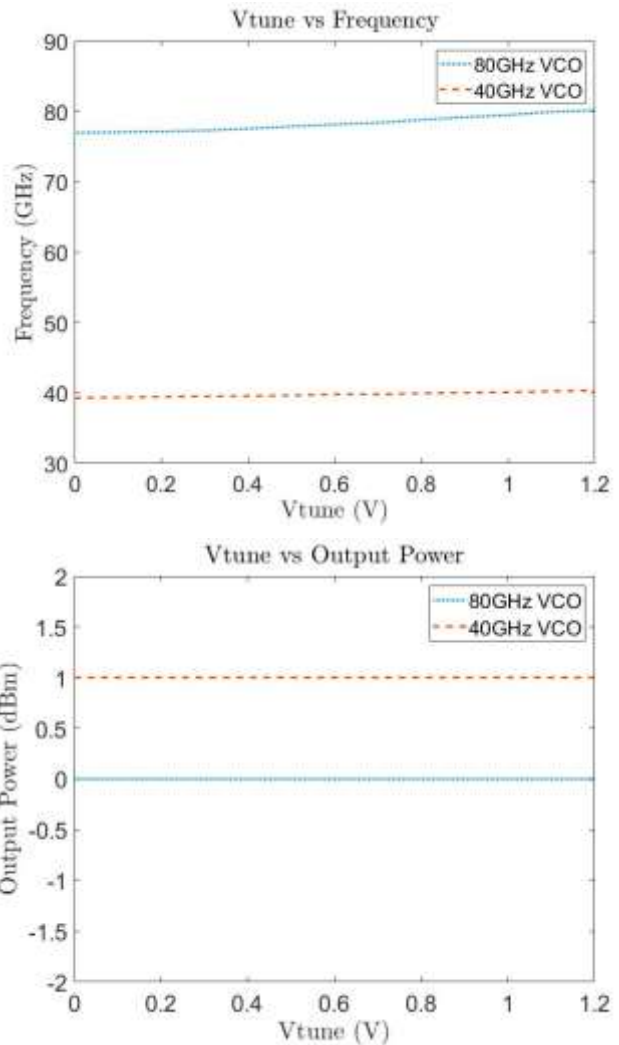


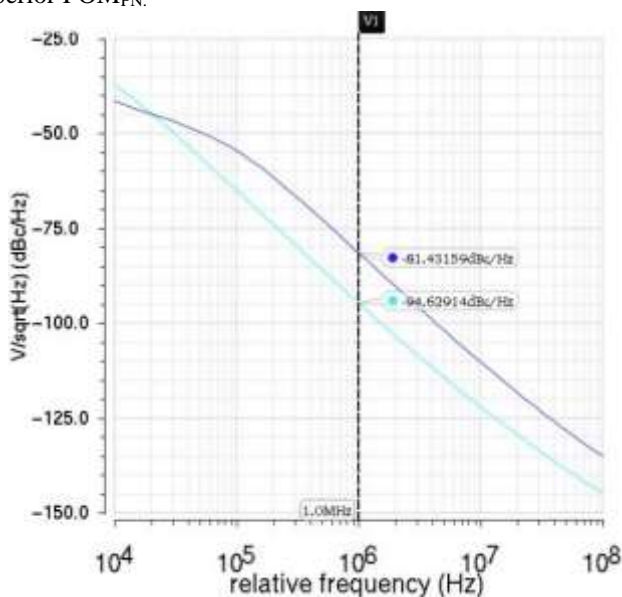
Fig. 7. Tuning range for both VCO₁ and VCO₂ w.r.t tuning voltages

Fig. 8. Output power for both VCO₁ and VCO₂ w.r.t tuning voltages

The frequency spectrum for both VCO modes can be seen in Fig. 6 and it is also verifying the results of Fig. 4 and Fig. 5. The tuning range of output frequency and output power of output signal are also plotted w.r.t tuning voltage in Fig. 7 and Fig. 8 respectively.

The phase noise is the most important parameter of an oscillator and it is necessary to illustrate phase noise for both modes of VCO and it is shown in Fig. 9 with reasonable phase noise of -94.62 dBc/Hz and -81.43 dBc/Hz at 1MHz offset for VCO₁ and VCO₂ respectively.

Table 1 compares the performance with state-of-the-art dual band VCOs. For comparison, the figure of merit considering phase noise (FOM_{PN}) is used. The proposed VCO achieves superior FOM_{PN}.

Fig. 9. Phase noise for both VCO₁ and VCO₂ at offset of 1 MHz

IV. CONCLUSION

The implemented dual band VCO has been presented with 40 GHz and 80GHz output frequencies. Inductor switching using transistor and transistor-based varactors are implemented in this work. The low power consumption with 0 to 1 dBm output power is observed for both modes of VCO.

V. REFERENCES

- [1] M. Tanomura, Y. Hamada, S. Kishimoto, M. Ito, N. Orihashi, K. Maruhashi, and H. Shimawaki, "TX and RX front-ends for 60 GHz band in 90 nm standard bulk CMOS," in *IEEE Int. Solid-State Circuits Conf. Dig. Tech. Papers*, Feb. 2008, pp. 558–559.
- [2] S. T. Nicolson, P. Chevalier, B. Sautreuil, and S. P. Voinigescu, "Single-chip W-band SiGe HBT transceivers and receivers for doppler radar and millimeter-wave imaging," *IEEE J. Solid-State Circuits*, vol. 43, pp. 2206–2217, 2008.
- [3] K. Scheir, G. Vandersteen, Y. Rolain, and P. Wambacq, "A 57-to-66 GHz quadrature PLL in 45 nm digital CMOS," in *IEEE Int. Solid-State Circuits Conf. Dig. Tech. Papers*, Feb. 2009, pp. 494–495 and 495a.
- [4] J. Grzyb, Y. Zhao, and U. R. Pfeiffer, "A 288-GHz lens-integrated balanced triple-push source in a 65-nm CMOS technology," *IEEE J. Solid-State Circuits*, vol. 48, no. 7, pp. 1751–1761, Jul. 2013.
- [5] S. Shahramian *et al.*, "Design of a dual W- and D-band PLL," *IEEE J. Solid-State Circuits*, vol. 46, no. 5, pp. 1011–1022, May 2011.
- [6] K.-H. Tsai, L.-C. Cho, J.-H. Wu, and S.-I. Liu, "3.5 mW W-band frequency divider with wide locking range in 90 nm CMOS technology," in *Proc. IEEE Int. Solid-State Circuits Conf.*, Feb. 2008, pp. 466–467.
- [7] K. W. Tang, S. Leung, N. Tieu, P. Schvan, and S. P. Voinigescu, "Frequency scaling and topology comparison of millimeter-wave CMOS VCOs," in *Proc. IEEE Compound Semiconductor Integr. Circuit Symp.*, Nov. 2006, pp. 55–58.
- [8] S. Kang and A. M. Niknejad, "A 100GHz active-varactor VCO and a bidirectionally injection-locked loop in 65nm CMOS," in *Proc. IEEE Radio Freq. Integr. Circuits (RFIC) Symp.*, pp. 231 - 234, Jun. 2013.
- [9] J. Yin and H.C. Luong, "A 57.5–90.1-GHz Magnetically Tuned Multimode CMOS VCO," *IEEE J. Solid-State Circuits*, vol.48, no.8, pp.1851-1861, Aug. 2013.
- [10] J.-Y. Lee, S.-H. Lee, H. Kim and H.-K. Yu, "A 45-to-60 GHz two-band SiGe:C VCO for millimeter-wave applications," in *IEEE RFIC Symp.*, Jun. 2007, pp.709-712.
- [11] L. Wu, A. W. L. Ng, L. L. K. Leung and H. C. Luong, "A 24- GHz and 60 GHz Dual-band Standing-wave VCO in 0.13- μ m CMOS process," in *IEEE RFIC Symp.*, Jun. 2010, pp. 145-148.
- [12] Y. Chen, Y. Pei and D. W. Leenaerts, "A Dual-band LO Generation System using a 40 GHz VCO with a Phase Noise of -106.8 dBc/Hz at 1-MHz," in *IEEE RFIC Symp.*, 2013, pp.203-206.



Journal of Applied and Emerging Sciences by BUIITEMS is licensed under a [Creative Commons Attribution 4.0 International License](https://creativecommons.org/licenses/by/4.0/).